

MATHEMATICAL MODELLING OF FLOW OVER PERIODIC STRUCTURES

PETR BAUER¹

Abstract. We examine the influence of roofs’ shapes on the boundary layer of a simplified urban canopy by computing non-stationary Navier-Stokes flow over a periodic pattern. The solution is obtained by means of finite element method (FEM). We use non-conforming Crouzeix-Raviart elements for velocity and piecewise constant elements for pressure. The resulting linear system is solved by the multigrid method. We present computational studies of the problem.

Key words. Incompressible flow, finite element method, Crouzeix-Raviart elements, multigrid, Vanka type smoothers

AMS subject classifications. 35K60, 35K65, 65N06, 68U10

1. Introduction. This paper deals with the flow over periodic patterns. Our primary motivation is modelling of the urban canopy, though other applications exist, including the modelling of rough surfaces in biology, or in the construction of pipelines.

Let $\Omega \subset \mathbb{R}^2$ be a polygonal domain derived from a rectangle by substitution of the bottom edge by a piecewise linear line representing the terrain. The boundary of Ω splits into four clearly defined parts, three of them being plain line segments. We will denote them by Γ_1 to Γ_4 in a counterclockwise fashion, or simply refer to them as the “terrain”, “outlet”, “upper”, and “inlet” parts; see Fig. 1.1.

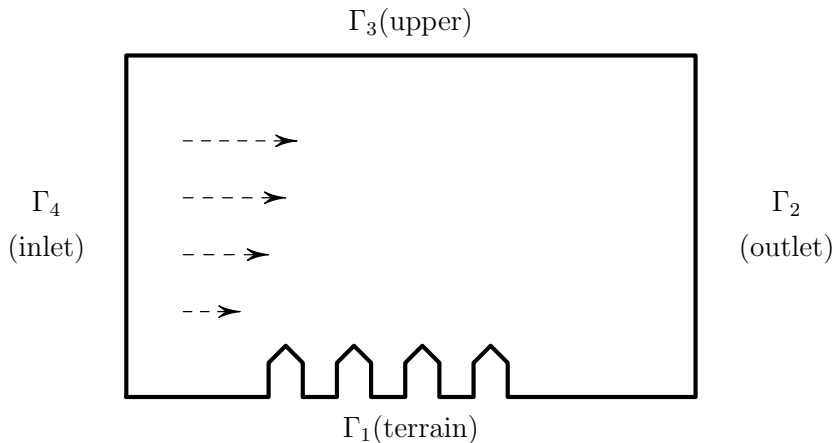


FIG. 1.1. *Computational domain*

We consider a periodic pattern of buildings with the basic parameters given by Fig. 1.2, and we examine the properties of the boundary layer depending on the roofs’ shape.

¹Institute of Thermomechanics, Academy of Sciences of the Czech Republic, Prague.

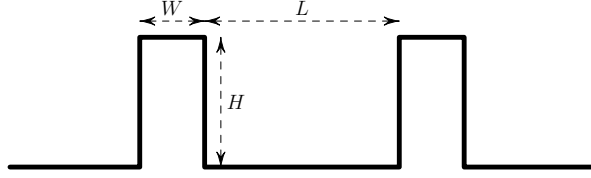


FIG. 1.2. Topology of a street canyon

On $[0, T] \times \Omega$, we solve the incompressible Navier-Stokes equations for velocity \vec{u} and pressure p , with the kinematic viscosity $\nu = 1.5 \cdot 10^{-5}$

$$\frac{\partial \vec{u}(t, \vec{x})}{\partial t} + \vec{u}(t, \vec{x}) \cdot \nabla \vec{u}(t, \vec{x}) - \nu \Delta \vec{u}(t, \vec{x}) + \nabla p(t, \vec{x}) = 0, \quad (1.1a)$$

$$\nabla \cdot \vec{u}(t, \vec{x}) = 0. \quad (1.1b)$$

The boundary conditions are of the Dirichlet and do-nothing type

$$u_x = u_z = 0 \quad \vec{x} \in \Gamma_1, \quad (1.2a)$$

$$-p\vec{n} + \nu(\nabla \vec{u}) \cdot \vec{n} = 0 \quad \vec{x} \in \Gamma_2, \quad (1.2b)$$

$$-p + \nu \frac{\partial u_x}{\partial z} = 0, u_z = 0 \quad \vec{x} \in \Gamma_3, \quad (1.2c)$$

$$\vec{u} = \vec{u}_{\text{in}} = (u_\alpha, 0) \quad \vec{x} \in \Gamma_4. \quad (1.2d)$$

The inlet profile u_α is given by the power law

$$u_\alpha(z) = \bar{u}_{ref} \left(\frac{z}{z_{ref}} \right)^\alpha, \quad (1.3)$$

where \bar{u}_{ref} is the average wind speed at some reference height z_{ref} , and α is the profile exponent.

As the initial condition $\vec{u}(0, \vec{x})$, we take the solution of the stationary Stokes problem, obtained by omitting the first two terms in (1.1a) and setting $\nu = 1.0$.

2. Weak formulation of Navier-Stokes equations. Let $X = (H^1(\Omega))^2$, $V(\vec{u}_{\text{in}}) = \{\vec{u} \in X, \text{ satisfying (1.2)}\}$, and $Q = L^2(\Omega)$. We set the following forms

$$a(\vec{u}, \vec{v}) = \nu \int_{\Omega} \sum_{i,j=1}^2 \left(\frac{\partial u_i}{\partial x_j} \frac{\partial v_i}{\partial x_j} \right) dx dz, \quad b(\vec{u}, \vec{v}, \vec{w}) = \int_{\Omega} \sum_{i,j=1}^2 \left(u_j \frac{\partial v_i}{\partial x_j} w_i \right) dx dz.$$

For time discretization, we use the semi-implicit Oseen scheme [2]. The time derivative is approximated by the backward Euler difference

$$\frac{\partial \vec{u}(t^n, x)}{\partial t} \approx \frac{\vec{u}^n - \vec{u}^{n-1}}{\tau}, \quad (2.1)$$

where $t^n = n\tau$. The convective term is discretized by $\vec{u}^{n-1} \cdot \nabla \vec{u}^n$, and the remaining terms are taken implicitly.

For each timestep t^n , we seek $\vec{u}^n \in V(\vec{u}_{\text{in}})$ and $p^n \in Q$, such that $\forall \vec{v} \in V(\vec{0})$ and $\forall q \in Q$

$$(\vec{u}^n, \vec{v}) + \tau b(\vec{u}^{n-1}, \vec{u}^n, \vec{v}) + \tau a(\vec{u}^n, \vec{v}) - \tau(p^n, \nabla \cdot \vec{v}) = (\vec{u}^{n-1}, \vec{v}), \quad (2.2)$$

$$(\nabla \cdot \vec{u}^n, q) = 0. \quad (2.3)$$

To deal with the nonlinear convective term, we employ the upwinding technique proposed by [3], and denote the respective approximation by $\bar{b}(\bar{u}_h^{n-1}, \bar{u}_h^n, \vec{v})$. The main idea of the method is to split the domain into lumped regions R_l around each midpoint Q_l of the original triangulation; see Fig. 2.1.

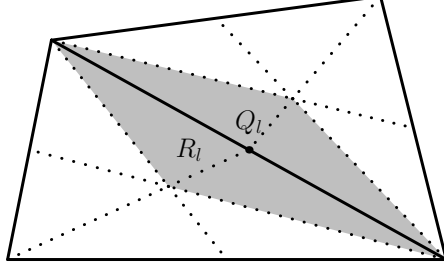


FIG. 2.1. Upwind - lumped region R_l (grey) around the midpoint Q_l

2.1. Discrete formulation. Let index h denote the respective finite-dimensional set $V^h(\bar{u}_{\text{in}})$, space Q^h , and the corresponding discrete functions \bar{u}_h^n, p_h^n . We introduce $\bar{w}_h \in V^h(\bar{u}_{\text{in}})$ to represent the inhomogeneous Dirichlet data, and we denote $\bar{v}_h = \bar{u}_h - \bar{w}_h \in V^h(\vec{0})$. The discrete problem for each timestep t^n reads: Find $\bar{v}_h^n \in V^h(\vec{0})$ and $p_h^n \in Q^h$, such that $\forall \vec{v} \in V^h(\vec{0})$ and $\forall q \in Q^h$

$$\begin{aligned} (\bar{v}_h^n, \vec{v}) + \tau \bar{b}(\bar{u}_h^{n-1}, \bar{v}_h^n, \vec{v}) + \tau a(\bar{v}_h^n, \vec{v}) - \tau (p_h^n, \nabla \cdot \vec{v}) &= \\ = (\bar{u}_h^{n-1} - \bar{w}_h^n, \vec{v}) - \tau \bar{b}(\bar{u}_h^{n-1}, \bar{w}_h^n, \vec{v}) - \tau a(\bar{w}_h^n, \vec{v}), \end{aligned} \quad (2.4)$$

$$(\nabla \cdot \bar{v}_h^n, q) + (\nabla \cdot \bar{w}_h^n, q) = 0.$$

2.2. Galerkin approximation. Let us denote the basis of $V^h(\vec{0})$ by $(\vec{\phi}_j^h)_{j \in J^h}$ and the basis of Q^h by $(\psi_k^h)_{k \in K^h}$. The functions \bar{v}_h and p_h can then be expressed as

$$\bar{v}_h^n = \sum_{j \in J^h} v_{h,j}^n \vec{\phi}_j^h, \quad p_h^n = \sum_{k \in K^h} p_{h,k}^n \psi_k^h. \quad (2.5)$$

We introduce the matrices

$$\mathbf{M} = (M_{ij})_{i,j=1}^{J^h}, \quad M_{ij} = (\vec{\phi}_i, \vec{\phi}_j), \quad (2.6)$$

$$\mathbf{A} = (A_{ij})_{i,j=1}^{J^h}, \quad A_{ij} = a(\vec{\phi}_i, \vec{\phi}_j), \quad (2.7)$$

$$\mathbf{B} = (B_{ij})_{i,j=1,1}^{J^h, K^h}, \quad B_{ij} = (\nabla \cdot \vec{\phi}_i, \psi_j), \quad (2.8)$$

$$\mathbf{N}(\bar{u}_h^{n-1}) = (N_{ij})_{i,j=1}^{J^h}, \quad N_{ij} = \bar{b}(\bar{u}_h^{n-1}, \vec{\phi}_i, \vec{\phi}_j), \quad (2.9)$$

and the coefficient vectors

$$\mathbf{v}_h^n = (v_{h,j}^n)_{j=1}^{J^h}, \quad \mathbf{p}_h^n = (p_{h,k}^n)_{k=1}^{K^h}. \quad (2.10)$$

Taking $\vec{v} = \vec{\phi}_i$ for $i = 1, \dots, J^h$ and $q = \psi_k$ for $k = 1, \dots, K^h$, the discrete formulation (2.4) leads to a system of linear equations for each timestep t^n

$$\mathbf{M} \mathbf{v}_h^n + \tau \mathbf{N}(\bar{u}_h^{n-1}) \mathbf{v}_h^n + \tau \mathbf{A} \mathbf{v}_h^n + \tau \mathbf{B}^T \mathbf{p}_h^n = \tilde{\mathbf{f}}, \quad (2.11a)$$

$$\mathbf{B} \mathbf{v}_h^n = \tilde{\mathbf{g}}, \quad (2.11b)$$

where

$$\tilde{f}_i = (\vec{u}_h^{n-1}, \vec{\phi}_i) - (\vec{w}_h^n, \vec{\phi}_i) - \tau \bar{b}(\vec{u}_h^{n-1}, \vec{w}_h^n, \vec{\phi}_i) - \tau a(\vec{w}_h^n, \vec{\phi}_i), \quad (2.11c)$$

$$\tilde{g}_k = -(\nabla \cdot \vec{w}_h^n, \psi_k). \quad (2.11d)$$

The matrices \mathbf{M} and \mathbf{A} are called the *mass matrix* and the *stiffness matrix* of the problem (2.11).

3. Numerical solution using FEM. We choose non-conforming Crouzeix-Raviart elements [4] to approximate the components of velocity, Fig. 3.1, and piecewise constant elements for pressure.

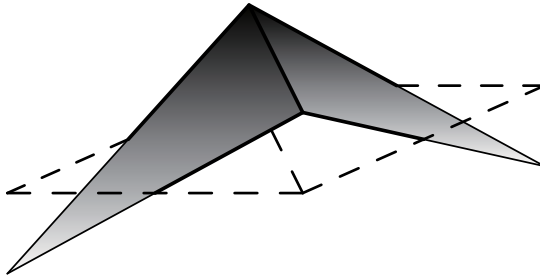


FIG. 3.1. *Crouzeix-Raviart element - scalar test function*

We use a hierarchy of uniformly refined structured meshes, Fig. 3.2, and employ a multigrid solver based on Vanka-type smoother [5] to solve the linear system (2.11). An extension for higher order elements can be found in [6].

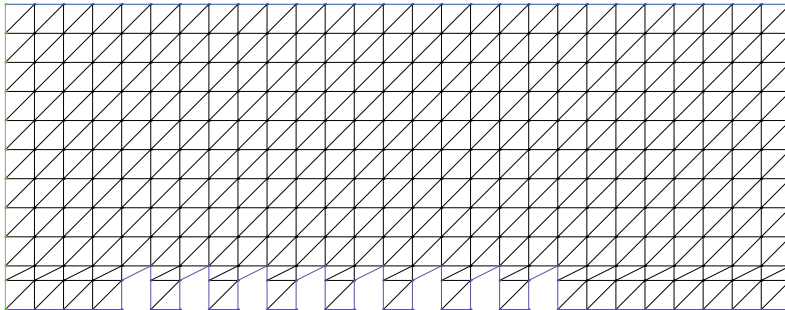


FIG. 3.2. *Coarsest mesh*

4. Experimental order of convergence. To verify the numerical scheme, we compute the experimental orders of convergence (EOCs) using an artificial problem with prescribed velocity field

$$\vec{u}_* = \cos(2\pi t) \begin{pmatrix} -x + 4y \\ -3x^2 + y \end{pmatrix}. \quad (4.1)$$

The problem is defined on a unit square with both the initial condition and the non-stationary Dirichlet boundary conditions given by (4.1). We evaluate the left-hand side of (1.1a) for \vec{u}_* and put it as an additional forcing term in the right-hand side of the system.

Solving the problem on two different grids M_1 and M_2 with space steps h_1 and h_2 respectively, we define the EOC for each time level as

$$EOC(t, M_1, M_2) = \log\left(\frac{\|\vec{u}_{h_1}(t) - \vec{u}_*(t)\|_{L_2(\Omega)}}{\|\vec{u}_{h_2}(t) - \vec{u}_*(t)\|_{L_2(\Omega)}}\right) / \log\left(\frac{h_1}{h_2}\right). \quad (4.2)$$

In our case, the coarsest mesh M_0 consists of four triangles obtained by cutting the square alongside both its diagonals. Through uniform refinement, we get M_1 , consisting of 16 triangles, and so on. The actual computations were done for four consecutive grids M_5 to M_8 , yielding three series of EOCs, which are shown in Fig. 4.1 for $t \in [0, 0.1]$.

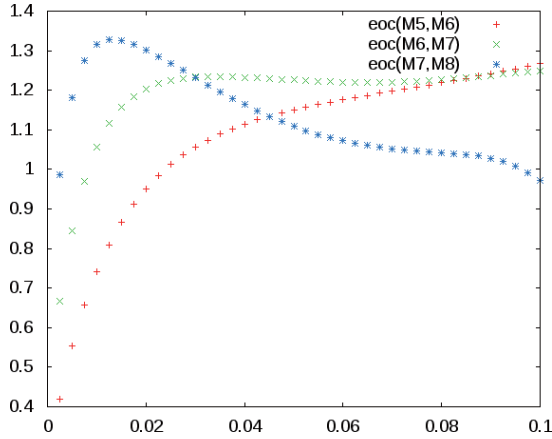


FIG. 4.1. *EOC series for $t \in [0, 0.1]$*

The EOCs of approximately one are mostly attributed to the inaccurate representation of the boundary condition. Currently, the function w_h is constructed as a combination of CR-type boundary elements.

5. Numerical results. We take a pattern consisting of eight buildings with square canyons between them and consider five different arrangements of roofs. The first one is a simple pattern with flat roofs. The next two configurations contain pitched roofs, one in the upwind direction and the other one in the downwind direction. The height of the pitched part is 0.5. We also examine an alternating pattern where the pairs of one higher building ($H = 1.5$) and one lower building ($H = 1.0$) periodically repeat. The Reynolds number is 10^5 in these four cases.

In the last simulation, we use symmetric saddle roofs with a relative height of 0.2. The Reynolds number is 5×10^4 in this case, and also the numerical parameters slightly differ. The complete set of parameters for all five cases is given in tables below.

PARAMETERS	cases (1), 2... , 4	DOFs	case 1	cases 2, ... , 4
domain size	$24 \times (8), 10.5$	velocity	5109056	7000896
Reynolds number	10^5	pressure	1703936	2334720
profile exponent	$\alpha = 0.28$			
initial flow	Stokes	τ	1/256	
time interval	$T = 60$	accuracy	1.0e-08	

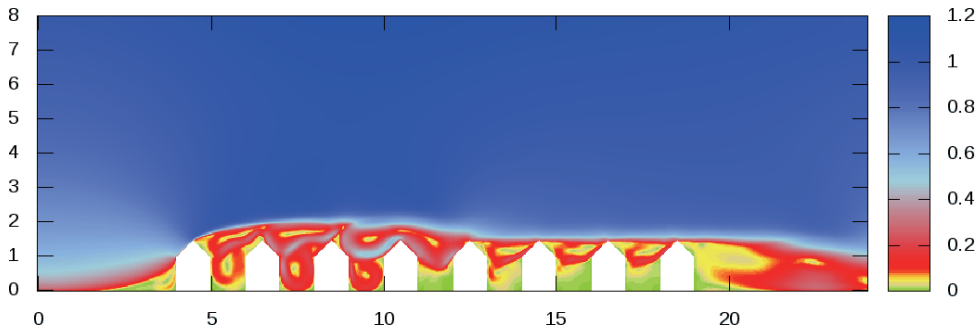


FIG. 5.1. $|\vec{u}(t)|$ at $t = 40$ for saddle roofs

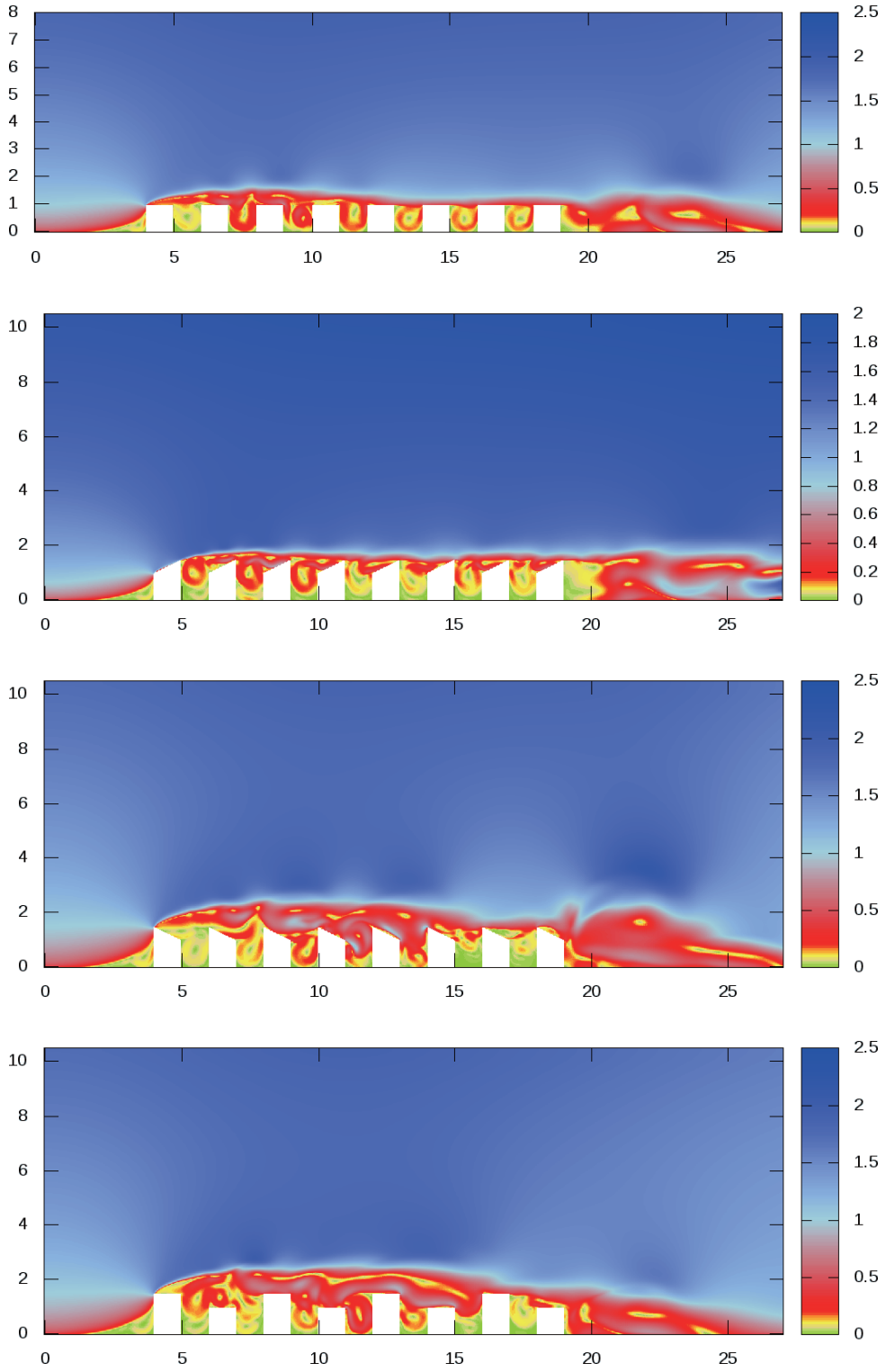
PARAMETERS	case 5	DOFs	case 5
domain size	24×8	velocity	4625920
Reynolds number	5×10^4	pressure	1540096
profile exponent	$\alpha = 0.28$		
initial flow	Stokes	τ	0.004
time interval	$T = 40$	accuracy	1.0e-08

The results are shown in Fig. 5.2 and Fig. 5.1. We can observe a clear difference depending on the type of the roofs, which is in agreement with what we would expect. The aerodynamical shape of the second arrangement creates a very thin boundary layer, while the third and fourth arrangement create a strongly turbulent layer. The saddle roofs produce pairs of vortices on top of each other.

6. Conclusion. We obtained some qualitative results of flow in a simplified urban canopy for different shapes of roofs. Our next goal is using a non-stationary inlet condition by [7] to catch the turbulent properties of the atmospheric boundary layer.

Acknowledgment. Our research on the flow over periodic structures was done in cooperation with the Institute of Thermomechanics of the Academy of Sciences of the Czech Republic.

Partial support of the project No. MSM 98-21000010 of the Ministry of Education of the Czech Republic is acknowledged.

FIG. 5.2. $|\vec{u}(t)|$ at $t = 55$ for cases 1, ..., 4

REFERENCES

- [1] F. BREZZI AND M. FORTIN. *Mixed and hybrid finite-element methods*. Springer Verlag, New York, 1991.
- [2] M. FEISTAUER. *Mathematical methods in fluid dynamics*. Longman, New York, 1993.
- [3] F. SCHIEWECK AND L. TOBISKA. An optimal order error estimate for upwind discretization of the Navier-Stokes equation. *Numerical methods in partial differential equations*, y.12 n.4:407–421, 1996.
- [4] M. CROUZEIX AND P.-A. RAVIART. Conforming and nonconforming finite element methods for solving the stationary Stokes equations I. *Rev. Franc. Automat. Inform. Rech. Operat.*, vol.7 R-3:33–76, 1973.
- [5] S.P VANKA. Block-implicit multigrid calculation of two-dimensional recirculating flows. *Computer Methods in Applied Mechanics and Engineering*, 59(1):29–48, 1986.
- [6] V. JOHN, P. KNOBLOCH, G. MATTHIES, AND L. TOBISKA. Non-Nested Multi-Level Solvers for Finite Element Discretisations of Mixed Problems. *Computing*, 68:313–341, 2002.
- [7] Z.-T. XIE AND I. P. CASTRO. Efficient generation of inflow conditions for large eddy simulation of street-scale flows. *Flow Turbulence Combust*, 81:449–470, 2008.